Electronic Supplementary Material (ESI) for Inorganic Chemistry Frontiers.

Electronic Supplementary Information

Completely suppressed high-voltage phase transition of P2/O3-$Na_{0.7}Li_{0.1}Ni_{0.1}Fe_{0.2}Mn_{0.6}O_2$ via Li/Ni co-doping for sodium storage

Figure S1

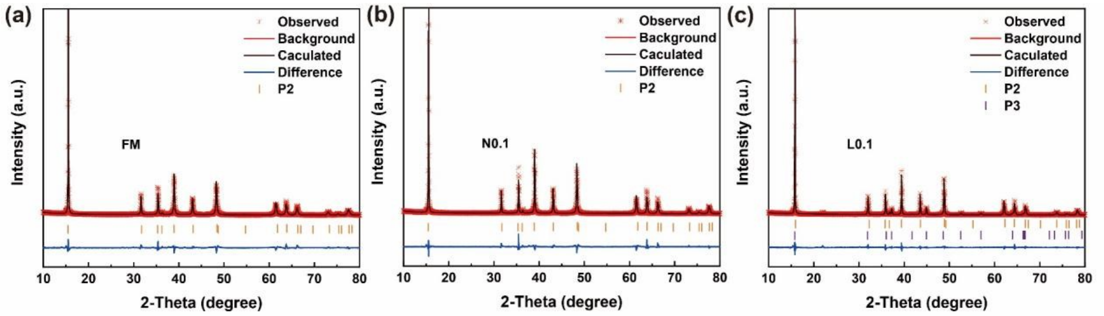

Fig. S1 XRD Rietveld refinements of (a) FM, (b) N0.1, (c) L0.1.

Figure S2

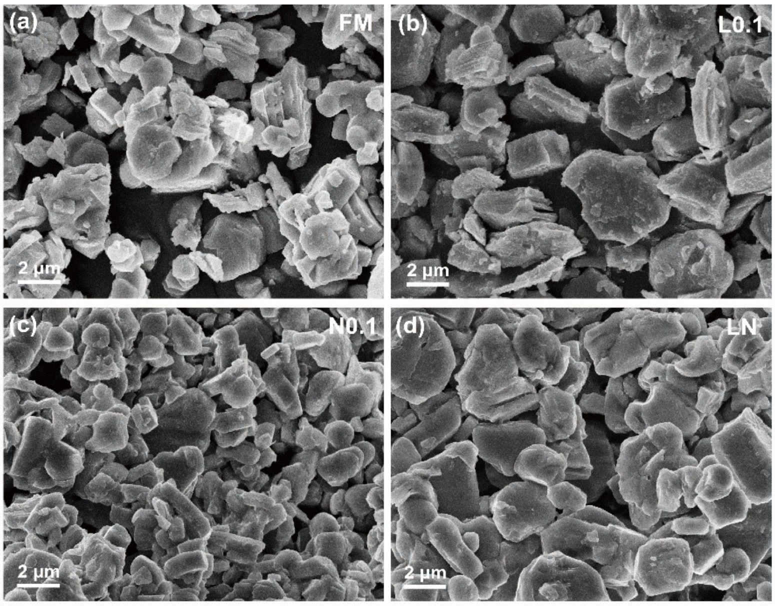

Fig. S2 SEM images of (a) FM, (b) L0.1, (c) N0.1, (d) LN.

Figure S3

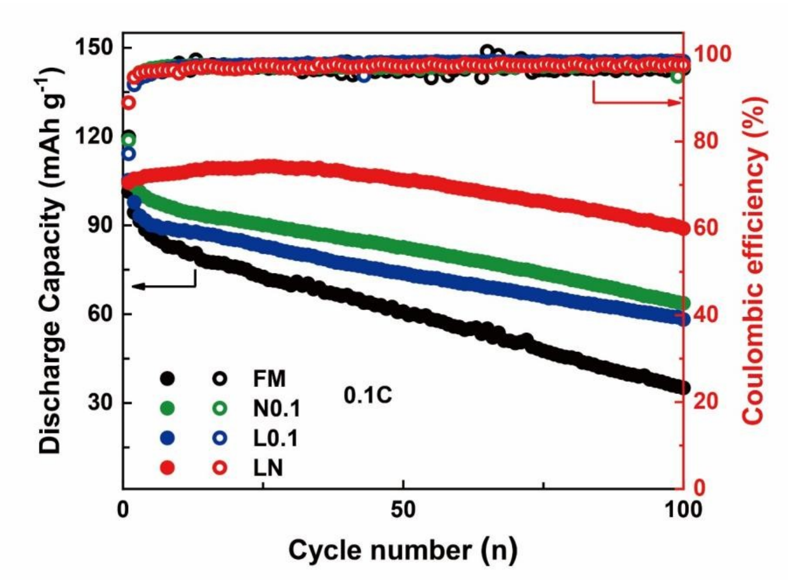

Fig. S3 Cycling performances of FM, L0.1, N0.1, and LN at 0.1C after 100 cycles.

Figure S4

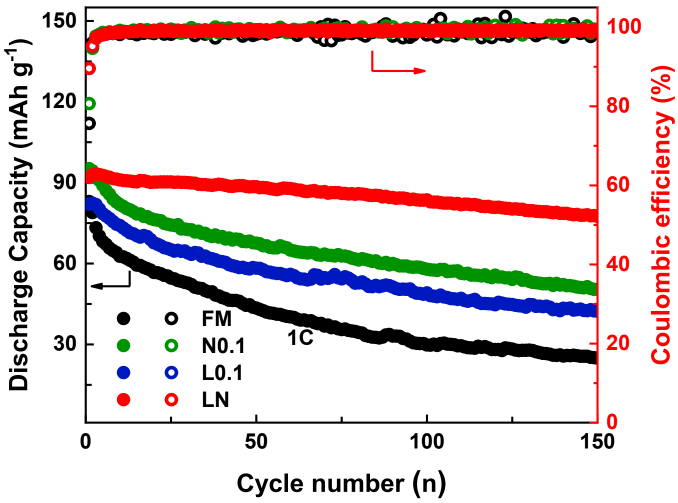

Fig. S4 Cycling performances of FM, L0.1, N0.1 and LN at 1C after 150 cycles.

Figure S5

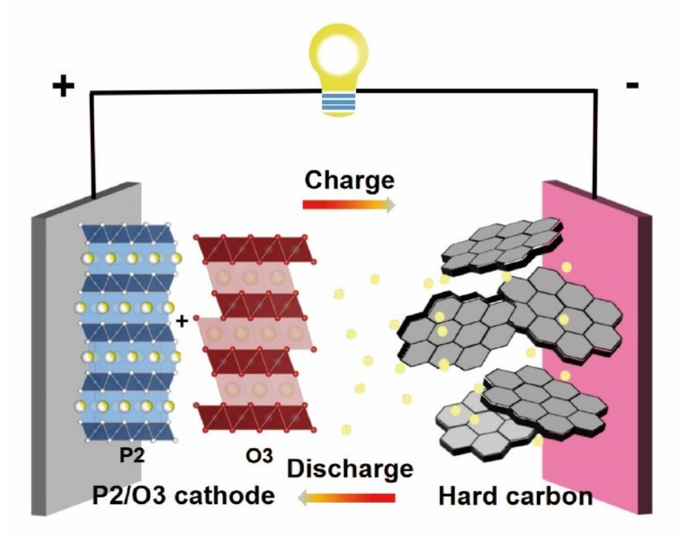

Fig. S5 Diagram of the LN||HC sodium-ion full battery.

Figure S6

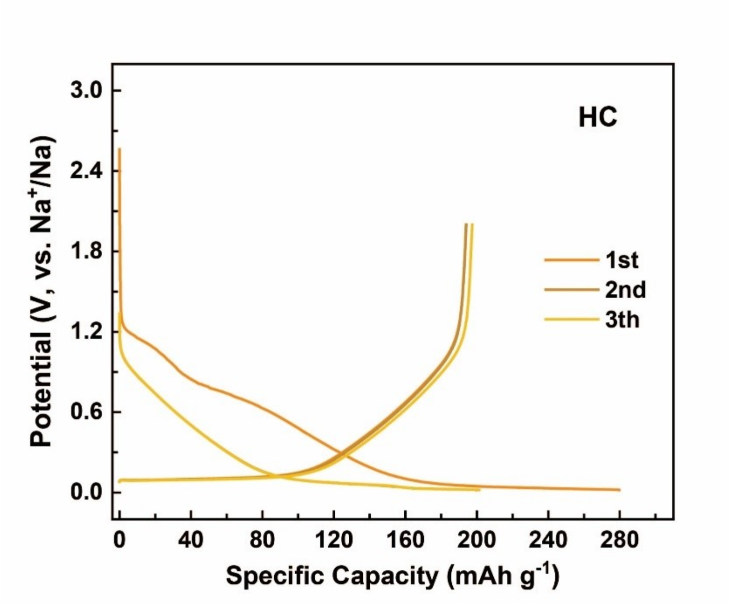

Fig. S6 Charge and discharge curves of hard carbon between 0.02 and 2 V at 0.1C ($1C = 300\ mA\ g^{-1}$).

Figure S7

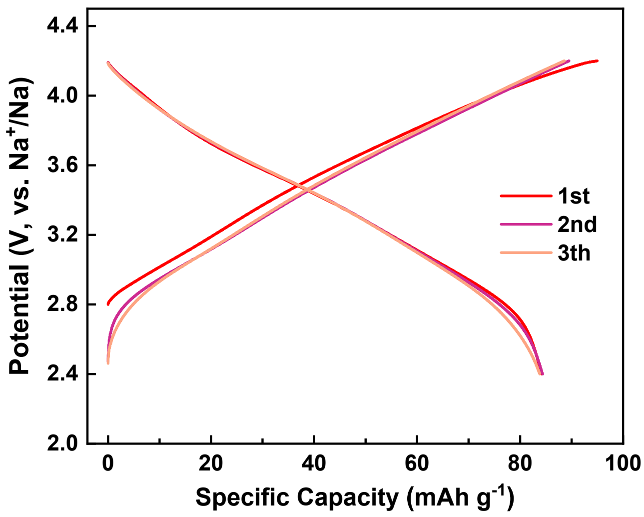

Fig. S7 The charge/discharge profiles of the full cell at 0.1C between 2.4–4.2V.

Figure S8

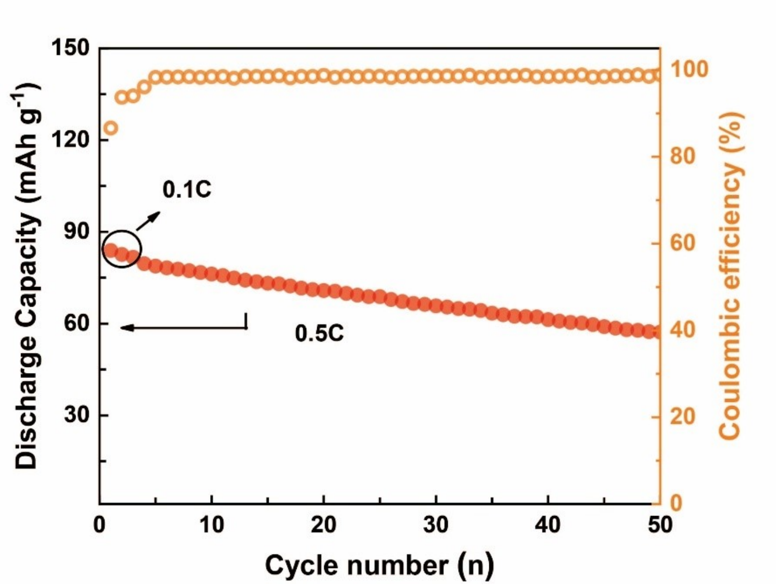

Fig. S8 Cycling performance of the full cell after 50 cycles at 0.5C.

Figure S9

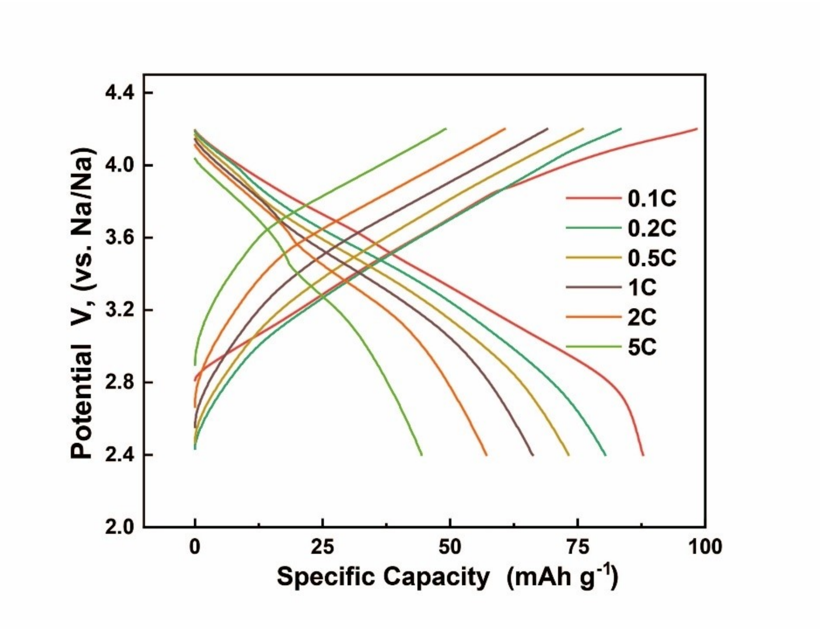

Fig. S9 Rate performance of the full cell at different current densities.

Figure S10

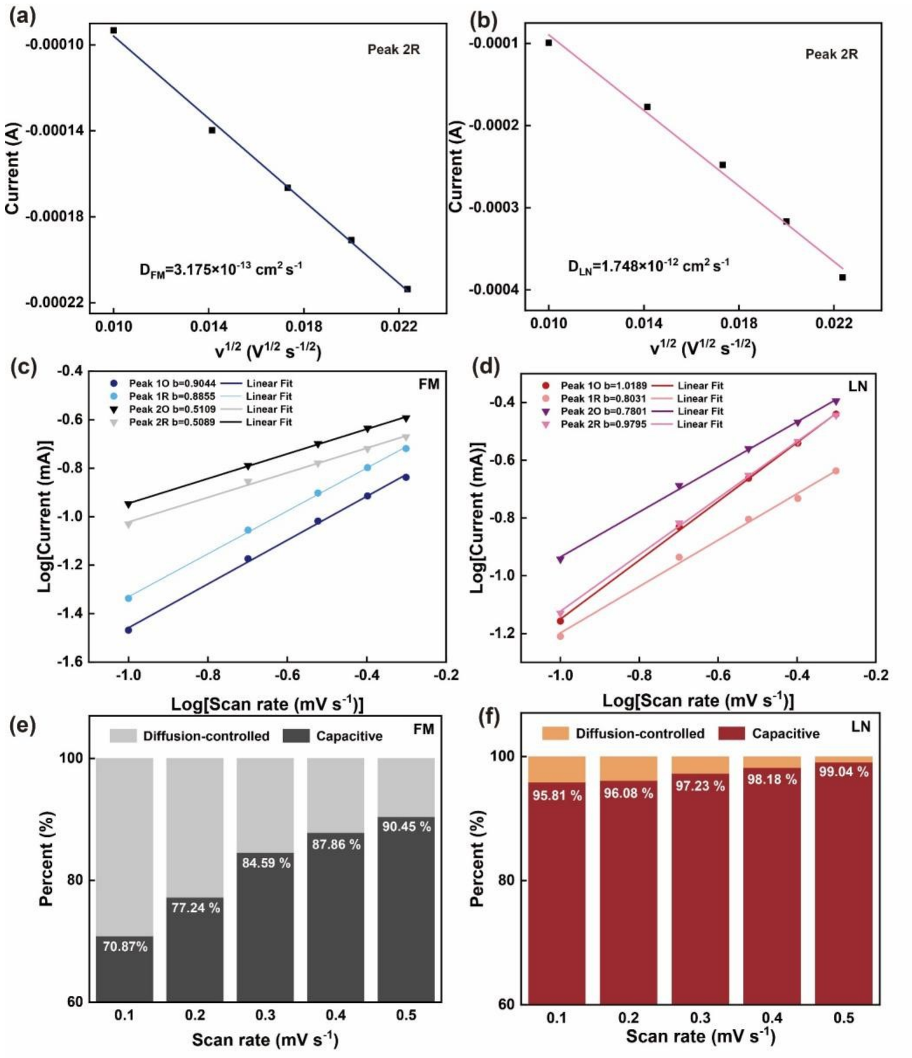

Fig. S10 Peak currents of 2R as a function of the square root of scan rate $v^{1/2}$ of (a) FM and (b) LN based on variable CV test. Linear relationships of log ip versus log v of (c) FM and (d) LN. Ratio of the pseudocapacitive and diffusion-controlled capacities at different scan rates of (e) FM and (f) LN.

Figure S11

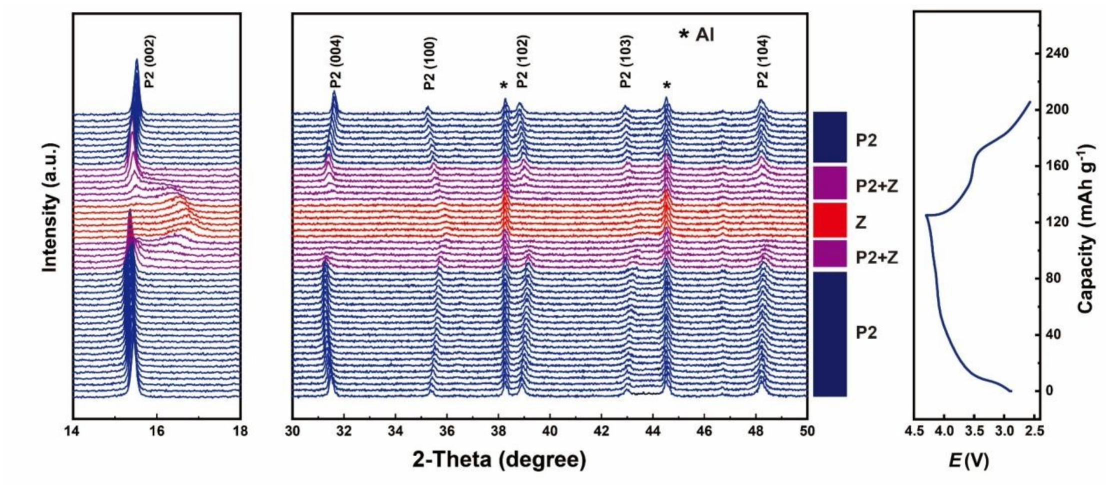

Fig. S11 *In-situ* XRD patterns collected during the first charge/discharge process of FM at 0.1C between 2.5 and 4.3 V.

Figure S12

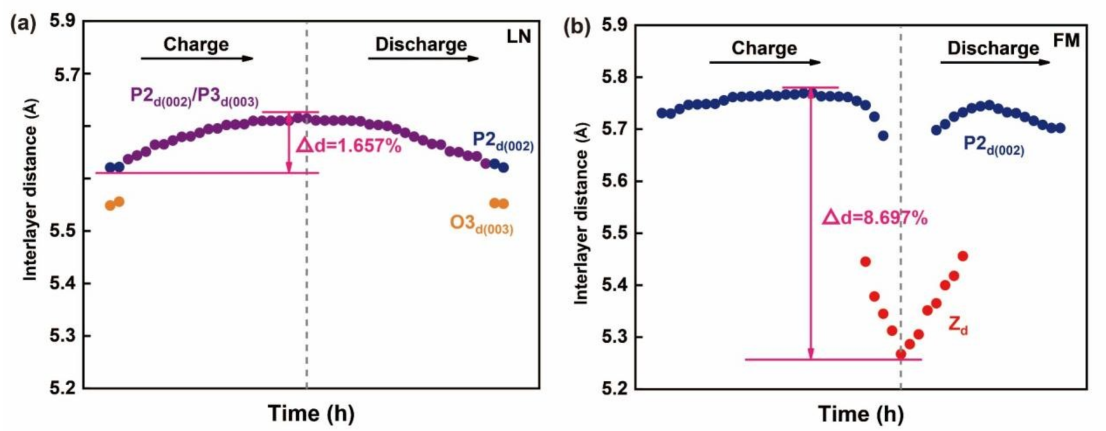

Fig. S12 Evolution of interlayer distances in (a) LN and (b) FM during the charge/discharge process.

Table S1

Structural parameters and atomic position of P2-FM from Rietveld refinement.

Atom	Site	x	y	z	Occ.
Na_f	2b	0.0000	0.0000	0.2500	0.2732
Na_e	2c	0.3333	0.6667	0.2500	0.4268
Fe	2a	0.0000	0.0000	0.0000	0.4000
Mn	2a	0.0000	0.0000	0.0000	0.6000
O	4f	0.6667	0.3333	0.0845	1.0000
a = 2.9099 Å		c = 11.2395 Å		V = 82.4213 $Å^3$	
R_p = 9.75 %	R_{wp} = 13.07 %	R_{exp} = 7.28 %	Chi2 = 3.92	Ratio:100%	

Table S2

Structural parameters and atomic position of P2 phase in P2/P3-L0.1 from Rietveld refinement.

Atom	**Site**	**x**	**y**	**z**	**Occ.**
Na_f	2b	0.0000	0.0000	0.2500	0.2826
Na_e	2c	0.3333	0.6667	0.2500	0.4174
Li	2a	0.0000	0.0000	0.0000	0.1000
Fe	2a	0.0000	0.0000	0.0000	0.3000
Mn	2a	0.0000	0.0000	0.0000	0.6000
O	4f	0.6667	0.3333	0.0859	1.0000
	a = 2.8908 Å		c = 11.1745 Å	V = 80.8757 Å^3	
R_p = 8.89 %	R_{wp} = 12.69 %		R_{exp} = 8.13 %	Chi2 = 2.43	Ratio:82.60%

Table S3

Structural parameters and atomic position of P3 phase in P2/P3-L0.1 from Rietveld refinement.

Atom	Site	x	y	z	Occ.
Na	3	0.0000	0.0000	0.1644	0.7000
Li	3	0.0000	0.0000	0.0000	0.1000
Fe	3	0.0000	0.0000	0.0000	0.3000
Mn	3	0.0000	0.0000	0.0000	0.6000
O1	3	0.0000	0.0000	0.6110	1.0000
O2	3	0.0000	0.0000	-0.6110	1.0000
a = 2.9087 Å		c = 16.8421 Å		V = 123.4112Å^3	
R_p = 8.89 %	R_{wp} = 12.69 %	R_{exp} = 8.13 %	Chi2 = 2.43	Ratio:17.40%	

Table S4

Structural parameters and atomic position of P2-N0.1 from Rietveld refinement.

Atom	Site	x	y	z	Occ.
Na_f	2b	0.0000	0.0000	0.2500	0.2422
Na_e	2c	0.3333	0.6667	0.2500	0.4578
Ni	2a	0.0000	0.0000	0.0000	0.1000
Fe	2a	0.0000	0.0000	0.0000	0.3000
Mn	2a	0.0000	0.0000	0.0000	0.6000
O	4f	0.6667	0.3333	0.0853	1.0000
a = 2.9049 Å		c = 11.2376 Å		V = 82.1278 $Å^3$	
R_p = 8.95 %	R_{wp} = 12.38 %	R_{exp} = 6.60 %	Chi2 = 3.50	Ratio:10%	

Table S5

Structural parameters and atomic position of P2 phase in P2/O3-LN from Rietveld refinement.

Atom	Site	x	y	z	Occ.
Na_f	2b	0.0000	0.0000	0.2500	0.2630
Na_e	2c	0.3333	0.6667	0.7500	0.4370
Li	2a	0.0000	0.0000	0.0000	0.1000
Ni	2a	0.0000	0.0000	0.0000	0.1000
Fe	2a	0.0000	0.0000	0.0000	0.2000
Mn	2a	0.0000	0.0000	0.0000	0.6000
O	4f	0.6667	0.3333	0.0923	1.0000
a = 2.8933 Å		c = 11.1003 Å		V = 80.4825Å^3	
R_p = 9.02 %	R_{wp} = 12.32 %		R_{exp} = 6.81 %	Chi2 = 4.54	Ratio:84.50%

Table S6

Structural parameters and atomic position of O3 phase in P2/O3-LN from Rietveld refinement.

Atom	Site	x	y	z	Occ.
Na	3a	0.0000	0.0000	0.0000	0.7000
Li	3b	0.0000	0.0000	0.0000	0.1000
Ni	3b	0.0000	0.0000	0.5000	0.1000
Fe	3b	0.0000	0.0000	0.0000	0.2000
Mn	3b	0.0000	0.0000	0.5000	0.6000
O	6c	0.0000	0.0000	0.2306	1.0000
a = 2.9266Å		c = 16.4721 Å		V = 122.1853 $Å^3$	
R_p = 9.02 %	R_{wp} = 12.32 %	R_{exp} = 6.81 %	Chi2 = 4.54	Ratio:15.54%	

Table S7

Comparison of electrochemical performance between different coatings modified-layered cathode materials for SIBs.

Material	Capacity /mA h g^{-1}	Capacity retention	Ref.
P2-$Na_{0.7}[Cu_{0.2}Fe_{0.2}Mn_{0.6}]O_2$	82.2 (2.5-4.2 V, 0.1C)	80% (80 cycles, 0.2C)	1
P2-$Na_{0.65}Li_{0.08}Cu_{0.08}Fe_{0.24}Mn_{0.6}O_2$	78 (2.5-4.2 V, 0.1C)	88.2% (500 cycles, 2C)	2
P2-$N_{a0.67}Fe_{0.4}Ti_{0.1}Mn_{0.5}O_2$	170 (1.5-4.2 V, 0.05C)	84% (45 cycles, 0.05C)	3
P2-$Na_{0.67}Mn_{0.65}Fe_{0.2}Ni_{0.15}O_2$	208 (1.5-4.3 V, 0.05C)	71% (50 cycles, 0.05C)	4
P2-$Na_{0.75}Ca_{0.05}Li_{0.15}Fe_{0.2}Mn_{0.6}O_2$	183 (1.5-4.3 V, 0.1C)	76% (150 cycles, 1C)	5
O3-$Na_{0.9}[Cu_{0.22}Fe_{0.30}Mn_{0.48}]O_2$	98 (2.5-4.05V, 0.1C)	97% (100 cycles, 0.2C)	6
O3-$NaFe_{0.55}Mn_{0.44}Nb_{0.01}O_2$	127 (2.0-4.0 V, 0.1C)	80% (100 cycles, 0.1C)	7
O3-$NaFe_{0.4}Mn_{0.49}Cu_{0.1}Zr_{0.01}O_2$	147.5 (2.0-4.10V, 0.1C)	69.6% (100 cycles, 0.2C)	8
P2/O3-$Na_{0.67}Li_{0.11}Fe_{0.36}Mn_{0.36}Ti_{0.17}O_2$	~150 (2.0-4.2 V, 1C)	85.4% (100 cycles, 1C)	9
P2/O3-$Na_{0.67}Fe_{0.425}Mn_{0.425}Mg_{0.15}O_2$	98.1 (1.5-4.2 V, 0.1C)	87.7% (100 cycles, 1C)	10
P2/O3-$Na_{0.7}Li_{0.1}Ni_{0.1}Fe_{0.2}Mn_{0.6}O_2$	102.2 (2.5-4.3 V, 0.1C)	74.6% (500 cycles, 10C)	**This work**

References:

1. S. Xu, J. Wu, E. Hu, Q. Li, J. Zhang, Y. Wang, E. Stavitski, L. Jiang, X. Rong, X. Yu, W. Yang, X.-Q. Yang, L. Chen and Y.-S. Hu, Suppressing the voltage decay of low-cost P2-type iron-based cathode materials for sodium-ion batteries, *J. Mater. Chem. A*, 2018, **6**, 20795-20803.
2. R. Qi, M. Chu, W. Zhao, Z. Chen, L. Liao, S. Zheng, X. Chen, L. Xie, T. Liu, Y. Ren, L. Jin, K. Amine, F. Pan and Y. Xiao, A highly-stable layered Fe/Mn-based cathode with ultralow strain for advanced sodium-ion batteries, *Nano Energy*, 2021, **88**, 106206.

3. J. K. Park, G. G. Park, H. H. Kwak, S. T. Hong and J. W. Lee, Enhanced rate capability and cycle performance of titanium-substituted P2-Type $Na_{0.67}Fe_{0.5}Mn_{0.5}O_2$ as a cathode for sodium-ion batteries, *ACS Omega*, 2018, **3**, 361-368.
4. D. Yuan, X. Hu, J. Qian, F. Pei, F. Wu, R. Mao, X. Ai, H. Yang and Y. Cao, P2-type $Na_{0.67}Mn_{0.65}Fe_{0.2}Ni_{0.15}O_2$ cathode material with high-capacity for sodium-ion battery, *Electrochim. Acta*, 2014, **116**, 300-305.
5. Y. Wang, X. Zhao, J. Jin, Q. Shen, N. Zhang, X. Qu, Y. Liu and L. Jiao, Low-cost layered oxide cathode involving cationic and anionic redox with a complete solid-solution sodium-storage behavior, *Energy Storage Mater.*, 2022, **47**, 44-50.
6. L. Mu, S. Xu, Y. Li, Y. S. Hu, H. Li, L. Chen and X. Huang, Prototype sodium-ion batteries using an air-stable and Co/Ni-free O3-layered metal oxide cathode, *Adv. Mater.*, 2015, **27**, 6928-6933.
7. L. Zhang, T. Yuan, L. Soule, H. Sun, Y. Pang, J. Yang and S. Zheng, Enhanced ionic transport and structural stability of Nb-doped O3-$NaFe_{0.55}Mn_{0.45-x}Nb_xO_2$ cathode material for long-lasting sodium-ion batteries, *ACS Appl. Energy Mater.*, 2020, **3**, 3770-3778.
8. Y. M. Zheng, X. B. Huang, X. M. Meng, S. D. Xu, L. Chen, S. B. Liu and D. Zhang, Copper and zirconium codoped O3-type sodium iron and manganese oxide as the cobalt/nickel-free high-capacity and air-stable cathode for sodium-ion batteries, *ACS Appl. Mater. Interfaces*, 2021, **13**, 45528-45537.
9. C. Chen, W. Huang, Y. Li, M. Zhang, K. Nie, J. Wang, W. Zhao, R. Qi, C. Zuo, Z. Li, H. Yi and F. Pan, P2/O3 biphasic Fe/Mn-based layered oxide cathode with ultrahigh capacity and great cyclability for sodium ion batteries, *Nano Energy*, 2021, **90**, 106504.
10. D. Zhou, W. Huang, X. Lv and F. Zhao, A novel P2/O3 biphase $Na_{0.67}Fe_{0.425}Mn_{0.425}Mg_{0.15}O_2$ as cathode for high-performance sodium-ion batteries, *J. Power Sources*, 2019, **421**, 147-155.